micromachines

MDPI

Article

A New Low-Temperature Solder Assembly Technique to Replace Eutectic Sn-Bi Solder Assembly

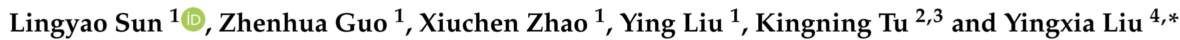

Lingyao Sun [1], Zhenhua Guo [1], Xiuchen Zhao [1], Ying Liu [1], Kingning Tu [2,3] and Yingxia Liu [4,*]

[1] School of Materials Science and Engineering, Beijing Institute of Technology, Beijing 100081, China; sunlingyao_513@163.com (L.S.); guozhenhua1318@163.com (Z.G.); zhaoxiuchen@bit.edu.cn (X.Z.); yingliu@bit.edu.cn (Y.L.)

[2] Department of Materials Science and Engineering, City University of Hong Kong, Hong Kong, China; kntu@cityu.edu.hk

[3] Department of Electrical Engineering, City University of Hong Kong, Hong Kong, China

[4] Department of Advanced Design and System Engineering, City University of Hong Kong, Hong Kong, China

* Correspondence: yingxliu@cityu.edu.hk

Abstract: We successfully achieved low-temperature assembly by reflowing the 13.5Sn-37.5Bi-45In-4Pb quaternary eutectic solder paste and the SAC 305 solder ball together at 140 °C for 5 min. The wetting angle of the mixed solder joint is 17.55°. The overall atomic percent of Pb in the mixed solder joint is less than 1%, which can be further reduced or eliminated. Moreover, after aging at 80 °C for 25 days, we observed no obvious decrease in shear strength of the fully mixed solder joint, which is the most advantage of this assembly technique over Sn58Bi solder assembly. The Bi phase segregation at the interface is slowed down compared with Sn-Bi solder joint. This low-temperature assembly is promising to be applied in advanced packaging technology to replace the eutectic Sn-Bi solder.

Keywords: low-temperature soldering; 3D IC; Bi aggregation; Sn-Bi solder

Citation: Sun, L.; Guo, Z.; Zhao, X.; Liu, Y.; Tu, K.; Liu, Y. A New Low-Temperature Solder Assembly Technique to Replace Eutectic Sn-Bi Solder Assembly. *Micromachines* **2022**, *13*, 867. https://doi.org/10.3390/mi13060867

Academic Editor: Wensheng Zhao

Received: 8 May 2022
Accepted: 25 May 2022
Published: 31 May 2022

Publisher's Note: MDPI stays neutral with regard to jurisdictional claims in published maps and institutional affiliations.

Copyright: © 2022 by the authors. Licensee MDPI, Basel, Switzerland. This article is an open access article distributed under the terms and conditions of the Creative Commons Attribution (CC BY) license (https://creativecommons.org/licenses/by/4.0/).

1. Introduction

As the downscaling trend of silicon chips is approaching its physical limits, advanced packaging technologies that integrate multiple chips, either vertically or horizontally, provide an alternative approach for developing post-Moore-era electronics [1–3]. The vertical or horizontal stacking of chips in advanced packaging technology requires a low-melting-point solder. Specifically, vertical stacking such as 3D integrated circuit (3D IC) is achieved via multiple reflows, and the use of a low-melting-point solder can prevent the re-melting of solder joints connected in a previous reflow [4]. In addition, packaging sizes generated by horizontal stacking are becoming increasingly large, leading to severe warpage problems [5]. This warpage can be relieved by using a low-melting-point solder during assembly. Thus, low-temperature assembly enables vertical and horizontal advanced packaging to be achieved, supporting continuing advances in microelectronic devices.

Currently, the packaging industry is trying to find an appropriate low-melting-point solder alloy. Tin–bismuth (Sn–Bi) eutectic solder has a melting point of 139 °C, but its brittleness limits its application in mobile electronic devices, especially after aging [6–12]. On the one hand, this is because aging causes Bi atom to segregate at the interface between the solder joint and the substrate [11,12]. As Bi is inherently brittle, this segregation increases the likelihood of interfacial fracture during drop testing. On the other hand, after aging, the IMC at the interface between the solder joint and the substrate will grow and thicken with the aging time. Due to the brittleness of the IMC, excessive thickness will reduce the mechanical properties and reliability of the joint [13–17]. In addition, the wettability of solder is also an important evaluation in electronic packaging industry. Since Bi will reduce the reaction speed of Sn and Cu, the wetting time will increase and the wettability will decrease [18]. Sn-Bi solder has very limited utility in mobile devices due to

its brittleness and poor wettability. Tin–indium (Sn-In) eutectic solder has a suitable melting point (118 °C), and bonds well with Cu, Ni, and Au substrates [19]. However, Sn-In solder is too soft, in addition, the widespread use of low-temperature solder with high In content is economically unfavorable because In is very expensive [20]. Most studies on low-melting-point solders have explored whether the addition of minor amounts of a third or fourth element into eutectic Sn-Bi alloys can produce alloys with better mechanical properties. These studies have not been successful, as the brittle nature of eutectic Sn–Bi has proven to be largely unmodifiable [21]. Additionally, there have been attempts to obtain a composite solder with better performance by mixing the two solders [22–27]; however, the reflow temperature is still high. Thus, there is an urgent need for a low-temperature assembly technology to replace eutectic Sn-Bi for use in industrial applications of mobile devices. In this paper, we report a low-temperature assembly technology to do so. Moreover, the assembled solder joint has a relatively stable shear test performance even after a long time of aging.

2. Experimental Section

The prepared Cu solder pads were ultrasonically cleaned with acetone, dilute hydrochloric acid, deionized water, and alcohol to remove surface oil and oxides. The Cu pads we used are 1 mm in diameter. And we developed a solder paste of 13.5Sn-37.5Bi-45In-4Pb quaternary eutectic alloy, which has a melting point of 60 °C. We use a low-temperature flux in the preparation of the 13.5Sn-37.5Bi-45In-4Pb solder paste, which is developed by the Beijing Institute of Nonferrous Metals and Rare Earth Applications. It works well in the range of 50~150 °C. The method of preparing the solder paste will be presented in our following paper. We printed the solder paste on the Cu pads with a designed stencil. A Sn96.5Ag3.0Cu0.5 (SAC305) solder ball was placed on each pad. The printed quaternary eutectic ultra-low-temperature solder paste is a cylinder of 1 mm in diameter and 100 μm in height. The SAC305 solder ball is 600 μm in diameter, as shown in Figure 1. Then, the substrate was reflowed at 100 °C, 120 °C, 140 °C, and 160 °C for 5 min. The reflowing temperature is higher than the melting point of 13.5Sn-37.5Bi-45In-4Pb solder paste and lower than the melting point of SAC305 solder balls. During reflow, the quaternary eutectic solder paste melts into a liquid state, while the SAC305 solder balls remain solid, which then gradually dissolve into the liquid solder. Figure 2 is a schematic diagram showing our low-temperature assembly strategy. After the reflow, we mounted and polished the samples to obtain cross-sectional images, which were observed by scanning electron microscope (SEM, Regulus 8230). The phase composition of the mixed solder before and after aging was determined by the energy dispersive spectrometer (EDS) and X-ray Diffractometer (XRD). The density of 13.5Sn-37.5Bi-45In-4Pb quaternary eutectic solder paste was measured by the Archimedes drainage method.

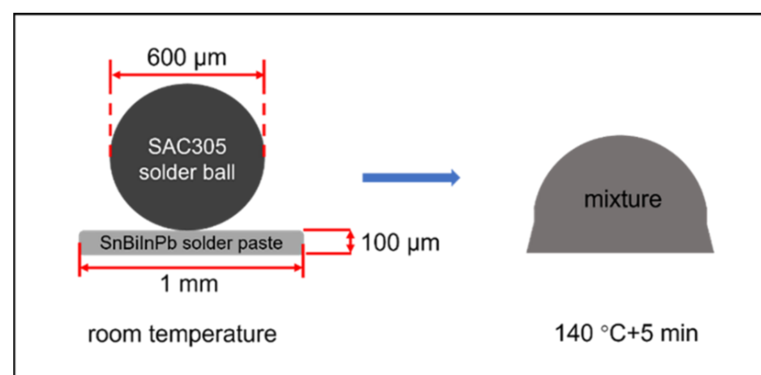

Figure 1. Schematic diagram of the assembly process using SAC305 solder balls and 13.5Sn-37.5Bi-45In-4Pb solder paste.

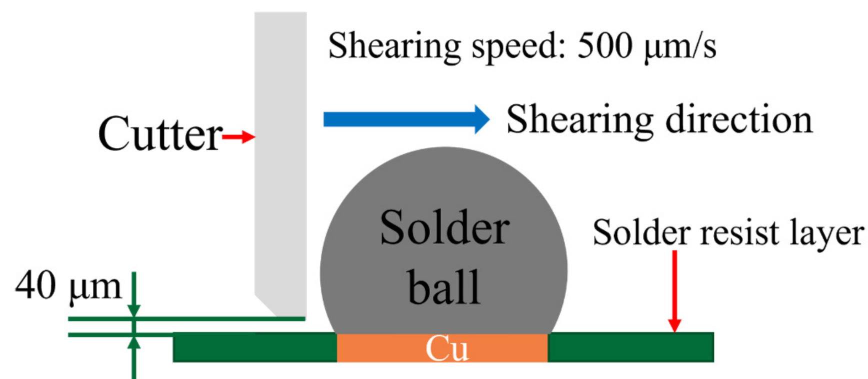

Figure 2. Schematic diagram of solder joint shear strength test.

The shear test was carried out on a PTR-1100 shear testing machine. The shear speed is 500 μm/s with a height of 40 μm, which is shown schematically in Figure 2. Additionally, 10 samples under each reflow condition were tested. The mixed solder bumps, obtained after reflowing at 140 °C for 5 min, were aged at 80 °C for 5 days, 15 days, and 25 days, respectively. Then, the microstructure of the aged solder joint was observed by SEM, and its phase composition was analyzed by EDS. We also tested the maximum shear strength of the fully mixed solder joint after aging by PTR-1100 shear testing machine.

3. Results and Discussion

3.1. Reflow Results

We choose a reflow temperature that is between the melting point of SAC305 (at 230 °C) and the melting point of 13.5Sn-37.5Bi-45In-4Pb solder paste (at 60 °C). The DSC curve of 13.5Sn-37.5Bi-45In-4Pb solder paste is shown in Figure 3. Therefore, solid–liquid inter-diffusion happens during the assembly process. During the solid–liquid inter-diffusion, Sn atoms from SAC305 solder ball will dissolve into the molten 13.5Sn-37.5Bi-45In-4Pb solder paste, and the two parts are mixed together. The fully mixed solder joint obtained after reflowing at 100 °C, 120 °C, 140 °C, and 160 °C for 5 min are shown in Figure 4. According to Figure 4a,b, there is still a clear boundary between the two parts after reflowing at 100 °C and 120 °C for 5 min, but a completely mixed and uniform solder bump is achieved after reflowing at 140 °C and 160 °C for 5 min.

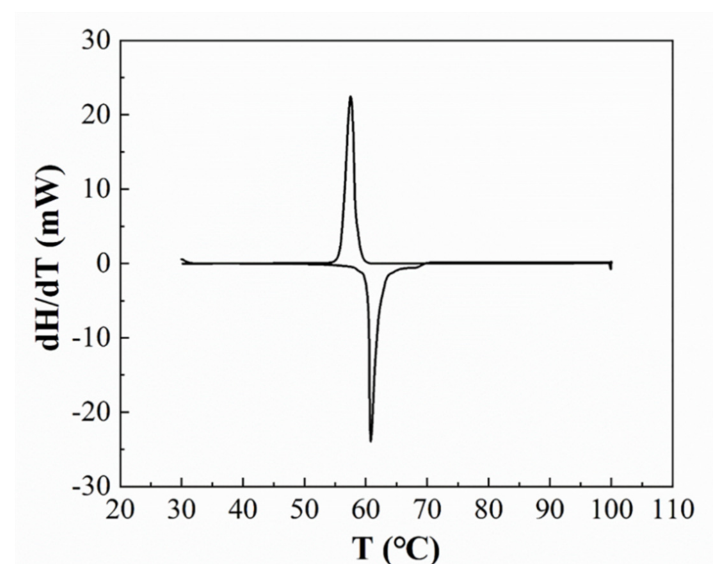

Figure 3. The DSC curve of 13.5Sn-37.5Bi-45In-4Pb solder paste.

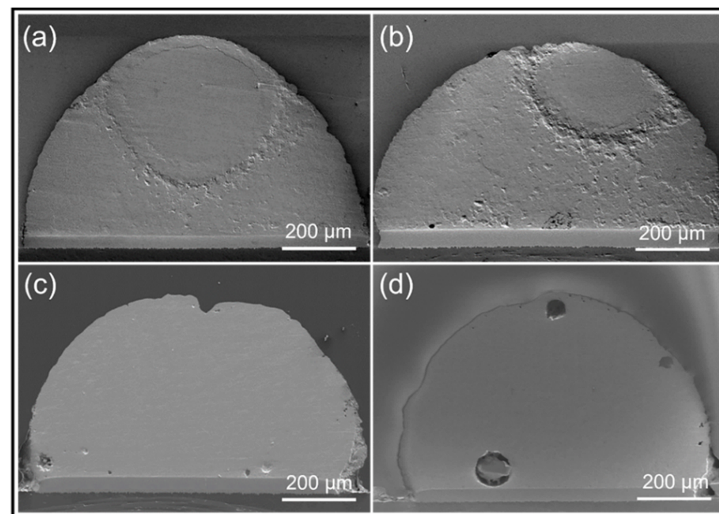

Figure 4. Overall SEM images of 13.5Sn-37.5Bi-45In-4Pb solder paste and SAC305 solder ball after reflowing at (**a**) 100 °C, (**b**) 120 °C, (**c**) 140 °C and (**d**) 160 °C for 5 min, respectively.

Higher magnification SEM images in Figure 5 show the uniformity of the microstructure after reflowing at 140 °C for 5 min. Figure 5a–f are the 500× magnification SEM images of the lower left, left, upper-left edge, upper right-edge, right, and lower right parts of the solder joint, respectively, and (g–i) are the 2000× enlarged view of the connection between the solder joint and the Cu plate, the middle and top of the solder joint. According to Figure 5, the composition of the mixed solder obtained after reflowing at 140 °C for 5 min is completely homogeneous. Therefore, 140 °C is considered the optimum temperature to obtain a fully mixed solder of 13.5Sn-37.5Bi-45In-4Pb and SAC305.

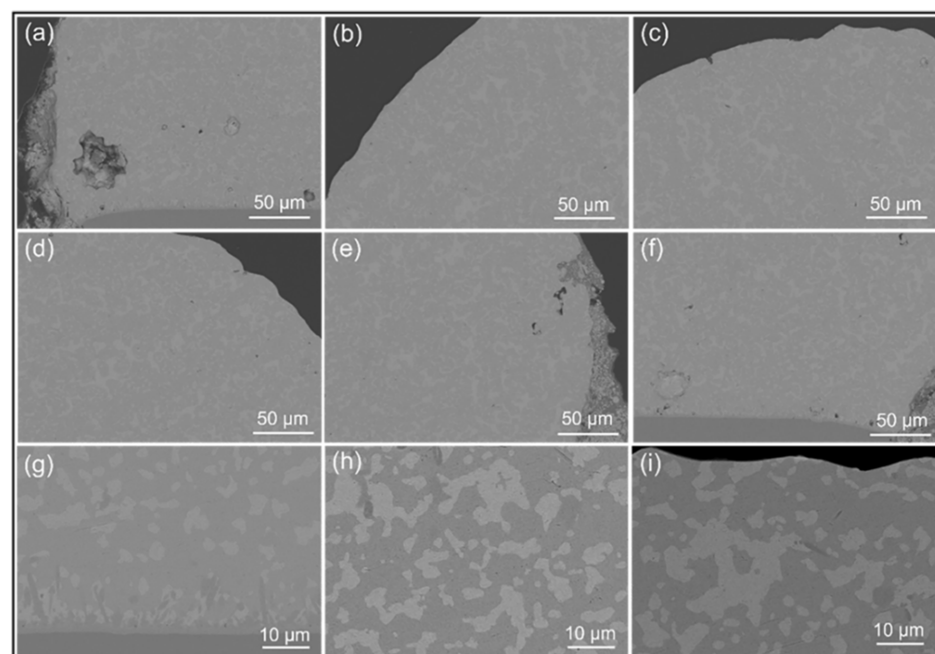

Figure 5. The fully mixed solder joint obtained after reflowing of 13.5Sn-37.5Bi-45In-4Pb solder and SAC305 at 140 °C for 5 min; (**a**–**f**): the 500× magnification of the lower left, left, upper-left edge, upper-right edge, right and lower right parts of the solder joint; (**g**–**i**): the 2000× enlarged view of the connection between the bottom of the solder joint and the Cu plate, the middle and top of the solder joint.

3.2. Composition of the Fully Mixed Solder Joint

We calculated the composition of the fully mixed solder joint with the value of volume and density. The volume of the solder paste and solder ball is calculated from the dimensions marked in Figure 1. The density of SAC305 solder balls is 7.37 g/cm^3 provided by the manufacturer, and the density of 13.5Sn-37.5Bi-45In-4Pb quaternary eutectic solder paste is 8.01 g/cm^3 tested by Archimedes drainage method. Then, the atomic percentage of each element is calculated and listed in Table 1.

Table 1. Calculation of the atomic percentage of each element in the fully mixed solder.

Elements	at. %
Ag	2.02
Cu	0.56
Sn	65.12
Bi	9.81
In	21.43
Pb	1.06

We performed the EDS mapping of the fully mixed solder joint after reflowing at 140 °C for 5 min, and the results are shown in Figure 6. Comparing the atomic percentage table in Figure 6 with Table 1, the difference in the content of each element is not significant and within the measurement error.

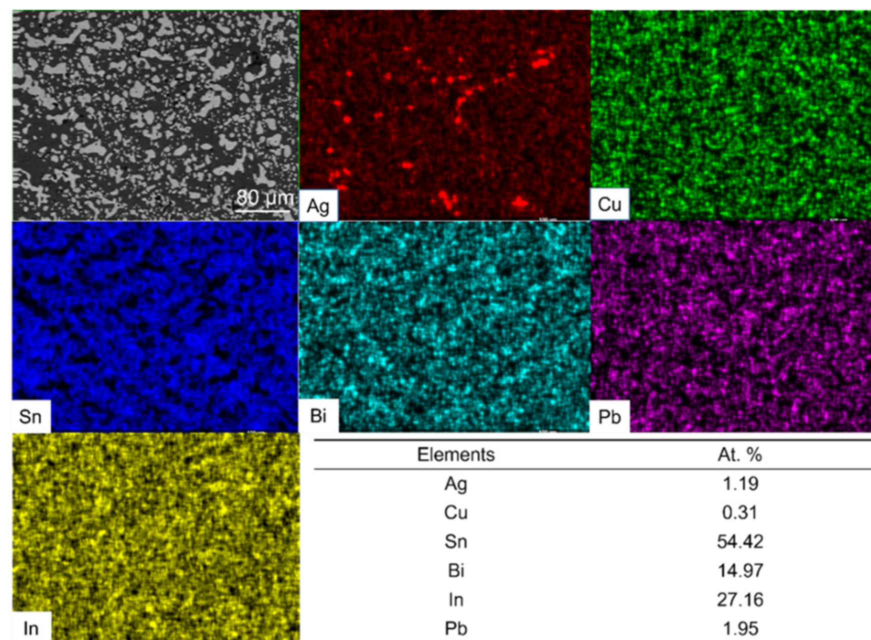

Elements	At. %
Ag	1.19
Cu	0.31
Sn	54.42
Bi	14.97
In	27.16
Pb	1.95

Figure 6. Elemental distribution and atomic percentage results of fully mixed composite solder joint.

From Figures 5 and 6, we can conclude that a well-mixed solder joint can be achieved by the 140 °C reflow of SAC305 solder ball and 13.5Sn-37.5Bi-45In-4Pb solder paste for 5 min. One thing that needs to be noted is the overall Pb atomic concentration in the mixed solder is about 1%. With further optimization, we can reduce the Pb atomic concentration to less than 0.5%. We can reduce the relative Pb content in the fully mixed solder by further reducing the amount of 13.5Sn-37.5Bi-45In-4Pb eutectic solder paste or increasing the amount of SAC305 solder. Specifically, this can be achieved by using thinner stencils (such as 50 μm, 30 μm) or by using larger diameter SAC305 solder ball. We will also try to reduce or even eliminate the Pb used in the low-melting-point solder paste. This means that the technology is promising to be applied to consumer products.

We further investigated the microstructure of the mixed solder joint after reflowing at 140 °C for 5 min with EDS and XRD, as shown in Figures 7 and 8 and Table 2. According to Figure 7 and Table 2, there are four phases in the mixed solder joint, including the Cu_6Sn_5, γ-phase, Bi_3In_5, and Ag_3Sn phases. The Cu_6Sn_5 phase is generated by the interfacial reaction between the solder joint and the Cu substrate, which is illustrated in the darkest area marked as region 1 in Figure 7. The γ-phase is a Sn-rich phase similar to the one marked in the Sn-In phase diagram shown in Figure 9a [28]. Bi_3In_5 is an intermetallic compound phase formed in the reaction between Bi and In [29,30], and so does Ag_3Sn, formed in the reaction between Ag and Sn [31]. Bi-In and Bi-Sn-In phase diagrams are shown in Figure 9b,c. All four phases are not pure and have substitutions from other elements. The XRD results in Figure 8 show that the two main phases in the mixed solder joint, Bi_3In_5 and γ-phase, are consistent with the EDS results [30]. The amount of Cu_6Sn_5 and Ag_3Sn phases is too little to be observed in the XRD results.

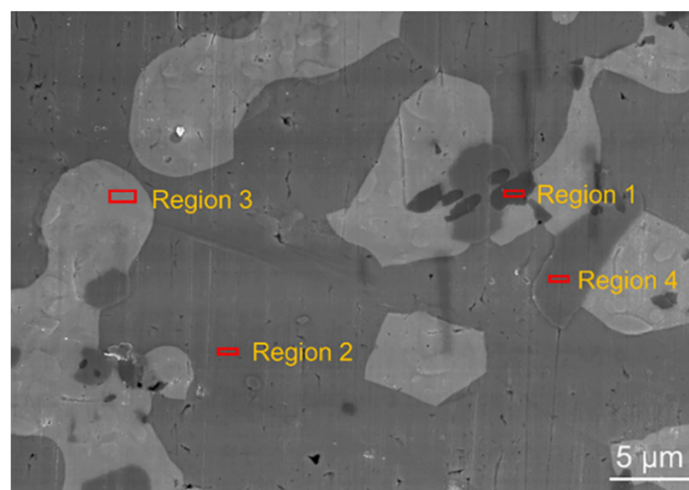

Figure 7. Local magnification SEM image of the fully mixed solder joint.

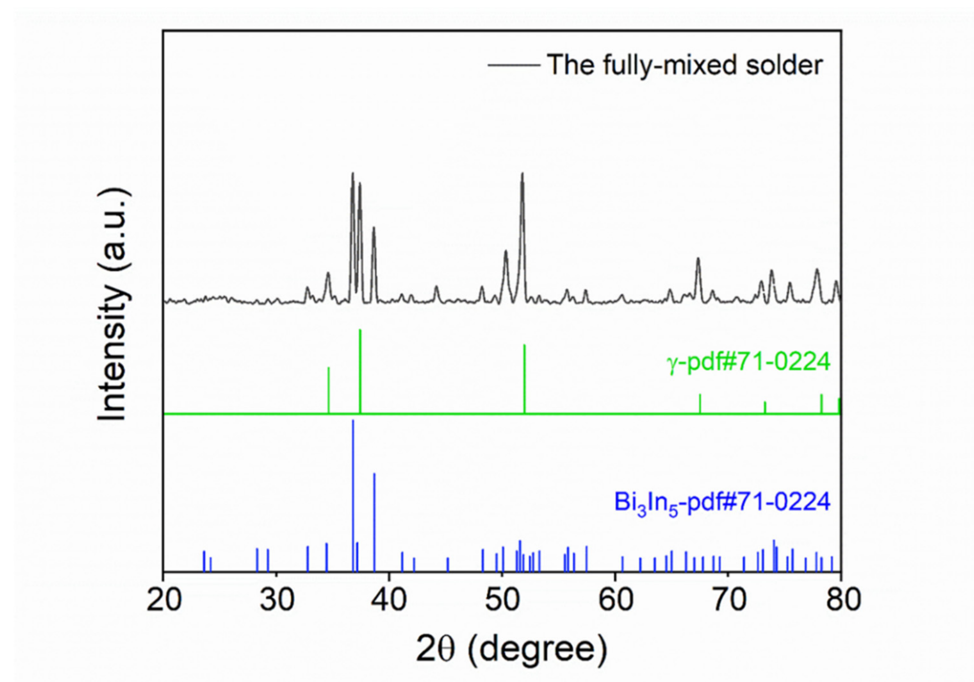

Figure 8. XRD analysis results of the mixed solder joint formed by SAC305 and 13.5Sn-37.5Bi-45In-4Pb after reflowing at 140 °C for 5 minutes.

Table 2. Element content of the regions marked in Figure 7.

Element / Atom (%) / Region	Sn	In	Bi	Pb	Ag	Cu	Phase
1	43.23	1.13	1.57	0.24	0.19	53.64	Cu_6Sn_5
2	78.02	17.23	3.82	0.58	0.35	-	γ
3	3.07	60.12	36.20	0.07	0.31	0.23	Bi_3In_5
4	23.84	9.63	0.39	0.28	65.86	-	Ag_3Sn

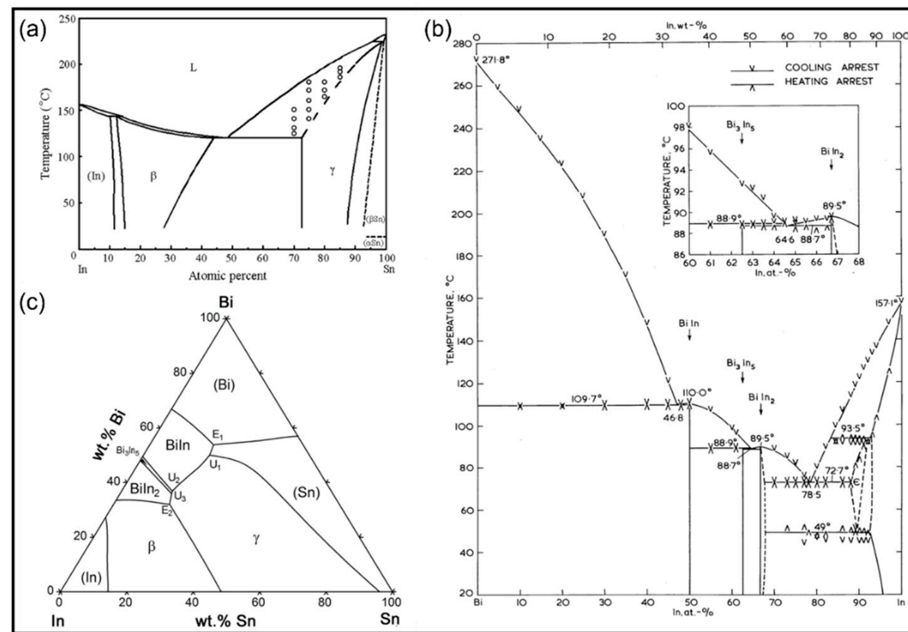

Figure 9. (**a**) The Sn-In phase diagram [28]; (**b**) the Bi-In phase diagram [29]; (**c**) the Bi-In-Sn phase diagram [30].

3.3. Wettability

To evaluate the wettability of composite solder joint where SAC305 solder ball is completely mixed with 13.5Sn-37.5Bi-45In-4Pb quaternary eutectic solder paste, we reflow the mixed solder directly on the cleaned Cu substrate. The wetting angle was measured, and that of SAC305 solder ball, Sn58Bi solder paste, and 13.5Sn-37.5Bi-45In-4Pb quaternary eutectic solder paste also were tested, respectively. The results are shown in Figure 10, where the four were compared. The wetting angle of the mixed solder is only 17.05°, while the wetting angles of the 13.5Sn-37.5Bi-45In-4Pb quaternary eutectic solder paste, SAC305 solder ball, and Sn58Bi solder paste are 26.82°, 24.24°, and 29.34°, respectively. Therefore, the wettability of our mixed solder is the most excellent among the four.

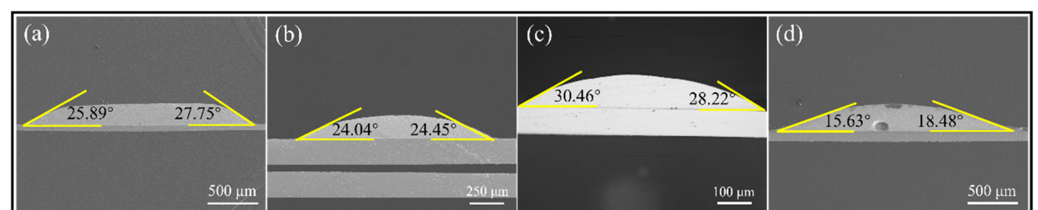

Figure 10. Wetting angle: (**a**) 13.5Sn-37.5Bi-45In-4Pb quaternary eutectic solder paste; (**b**) SAC305 solder ball; (**c**) Sn58Bi solder paste; (**d**) the fully mixed solder of 13.5Sn-37.5Bi-45In-4Pb quaternary eutectic solder paste and SAC305 solder ball.

3.4. Aging Performance of the Mixed Solder Joint

The solder bumps obtained after reflowing at 140 °C for 5 min were thermally aged at 80 °C for 5 days, 15 days, and 25 days [32]; the results are shown in Figure 11a–d. The thicknesses of intermetallic compounds (IMC) generated by the reaction between the mixed solder and the interface before aging and after aging for 5, 15, and 25 days were measured as 1.06 µm, 2.39 µm, 3.66 µm, and 4.08 µm, respectively, as shown in Table 3. The composition analysis of IMC before aging and after aging for 25 days was carried out using EDS, as shown in Figure 12. It was found that the IMC was $Cu_6(Sn, In)_5$, with In substitute some Sn atoms in Cu_6Sn_5 IMC.

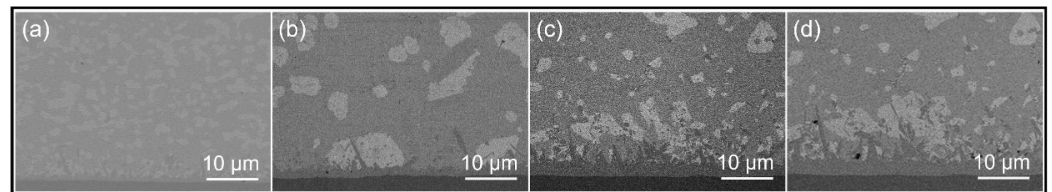

Figure 11. SEM images of the interface between the fully mixed solder joint and the Cu substrate: (**a**) before aging, (**b**) 5 days, (**c**) 15 days, and (**d**) 25 days of aging.

Table 3. The thickness of IMC of the fully mixed solder joints before aging and after aging for 5 days, 15 days, and 25 days.

Aging Time	The Average Thickness of IMC Layer (µm)
0 day	1.06
5 days	2.39
15 days	3.66
25 days	4.08

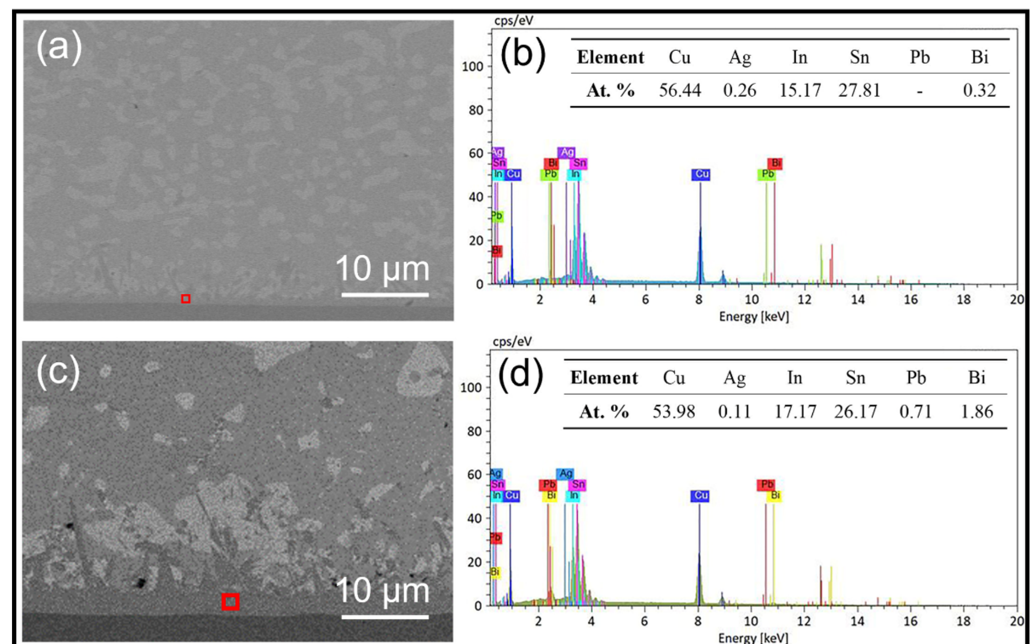

Figure 12. Composition analysis of IMC: (**a**) before aging and (**c**) after 25 days of aging: (**b**) EDS results of the region marked in (**a**); (**d**) EDS results of the region marked in (**c**).

After aging for 15 and 25 days, we observe the coarsening effect of Bi_3In_5 phase. We also observe slight aggregation of Bi_3In_5 phase at the interface. The aggregated phase of Bi_3In_5 is not continuous, which may be due to the spinous shape of intermetallic compound at the solder and Cu interface.

Figure 13 shows the EDS Mapping of the mixed solder joint after 25 days of aging. In Figure 13, the element distribution is uniform throughout the solder joint. Further comparison of the tables in Figures 6 and 13 shows that there are also no significant changes in the atomic percentage of the elements.

We put the results of XRD analysis before and after aging together for comparison, as shown in Figure 14. The main components of the phases before aging and after aging remain the same, which are the γ-phase and Bi_3In_5 phase. Figures 13 and 14 demonstrate that the microstructure of the mixed solder joint is stable after aging.

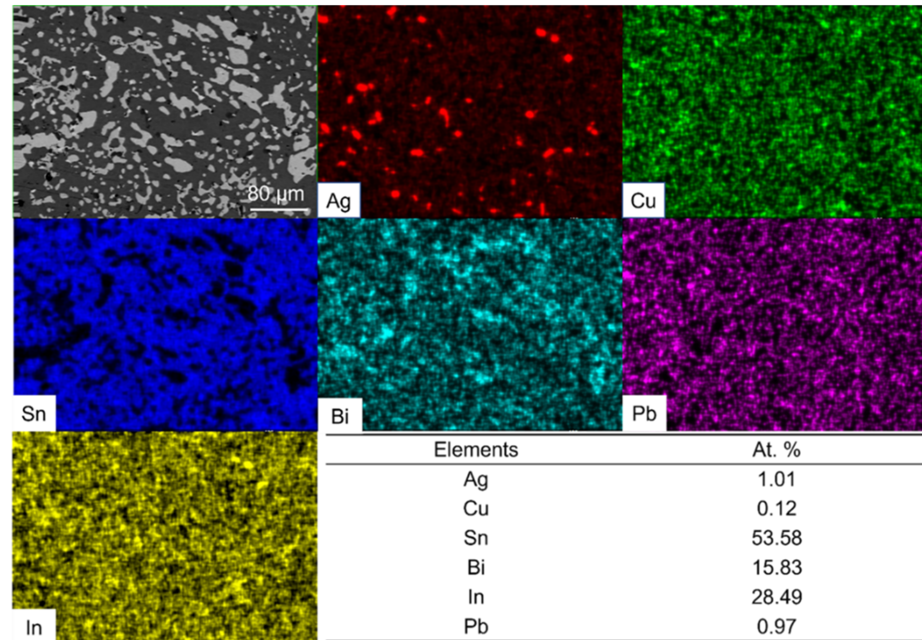

Elements	At. %
Ag	1.01
Cu	0.12
Sn	53.58
Bi	15.83
In	28.49
Pb	0.97

Figure 13. Elemental distribution and atomic percentage results of fully mixed solder joint after 25 days of aging.

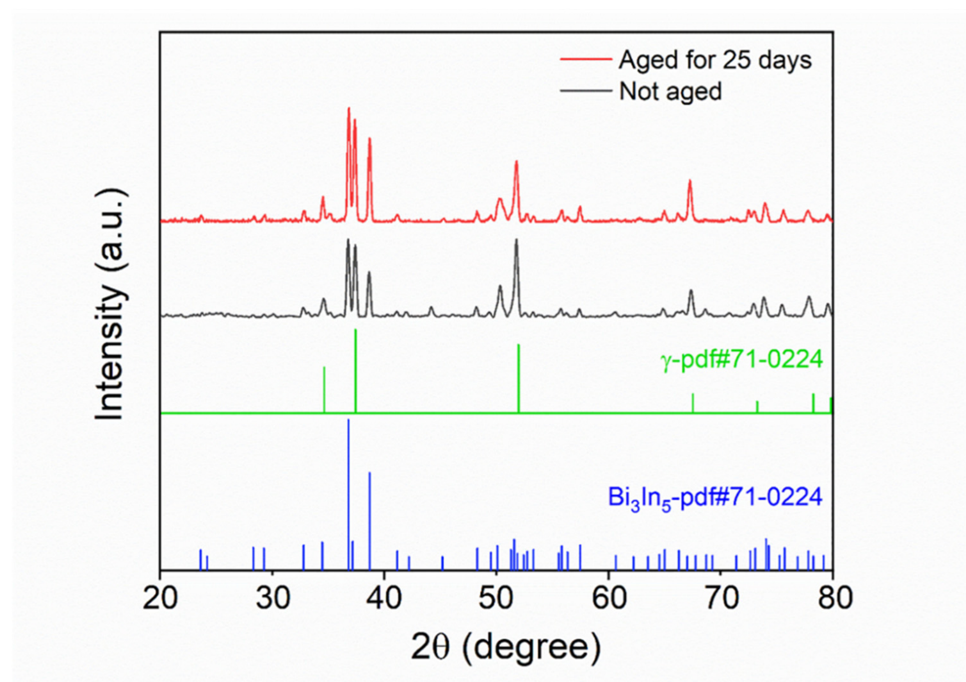

Figure 14. XRD analysis results of the mixed solder joint before and after aging for 25 days.

3.5. Shear Test of the Fully Mixed Solder Joint

The shear strength of the mixed solder joint was tested and compared with that of the original 13.5Sn-37.5Bi-45In-4Pb quaternary solder formed after reflowing at 140 °C for 5 min, as shown in Figure 15a. The shear strength of the original 13.5Sn-37.5Bi-45In-4Pb quaternary solder joint is only 17.62 (±1.57) MPa, while the mixed solder joint is 25.53 (±1.63) MPa, which was much higher than that of the original quaternary solder joint. In addition, the shear strength of SAC305 is 23 MPa [33], so the shear strength of the mixed solder is similar to SAC305.

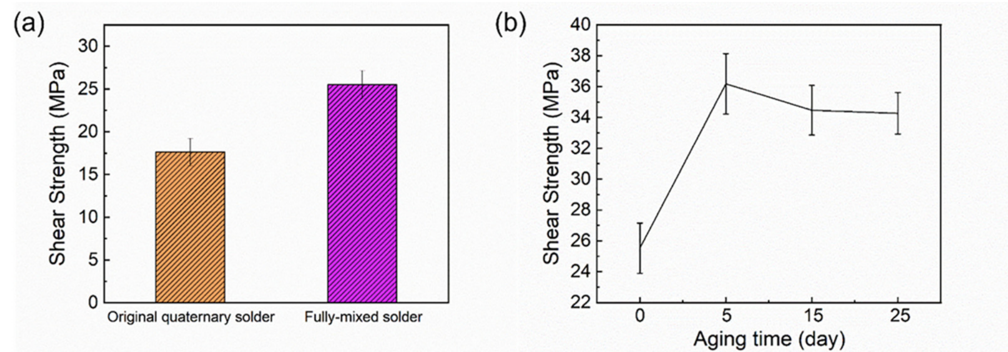

Figure 15. (**a**) Shear strength of the original quaternary solder joint and the fully mixed solder joint; (**b**) Variation of shear strength of fully mixed solder joint with aging time.

The shear strength of the samples after aging for 5, 15, and 25 days after reflowing at 140 °C for 5 min is shown in Figure 15b. The shear strength of the samples before aging was 25.53 (±1.63) MPa, and the shear strength of the samples after aging at 80 °C for 5, 15, and 25 days were 36.18 (±1.96) MPa, 34.47 (±1.61) MPa, and 34.27 (±1.34) MPa, respectively. After 5 days of aging, the shear strength is increased and there is almost no decrease in shear strength with increasing aging time. Because the thickness of the IMC has an important effect on the performance of the solder joint, the IMC needs to be thick enough to ensure a strong and reliable bonding. However, due to the brittleness of the IMC, if it is too thick it will also reduce the joint reliability [14,15,17]. After 5 days of aging, the shear strength increased due to the growth of IMC. Table 3 shows that although the IMC thickens after aging, it is not over-thickened, resulting in good shear strength. It has been shown that the thickness of IMC at the Sn58Bi/Cu interface increases linearly with the square root of the aging time [34–37], that is, the IMC growth at the interface in solder joint follows the empirical diffusion formula:

$$X = (Dt)^{\frac{1}{2}} + X_0 \quad (1)$$

where X is the total IMC thickness, X_0 is the initial IMC thickness, t is the aging time, and D is the diffusivity of the IMC layer [37]. The growth of IMC thickness $(X - X_0)$ is plotted with the square root of aging days $\left(t^{\frac{1}{2}}\right)$, and the results are shown in Figure 16. The growth of IMC with aging time for Sn58Bi was compared with published results [37]. The IMC growth rate of Sn58Bi aged at 135 °C was reported to be 3.0 μm/day$^{1/2}$, while the IMC growth rate of the fully mixed solder was only 0.623 μm/day$^{1/2}$, which is much less than that of Sn58Bi.

The Bi containing low melting temperature solder, which can keep a stable shear strength after aging, is an important finding in our work. Many works have reported the shear strength decrease in Bi containing solder after aging [32,38,39], which is due to the large aggregation of Bi at the interface between substrate and solder [12]. A continuous decrease in the shear strength was reported with an increase in aging time of 7 days, 14 days, and 21 days at an aging temperature of 100 °C. The total decrease of shear strength can be 30~40% after aging for 21 days [8]. In our work, we show a much better shear test

performance after aging. We tend to believe it is because the Bi atoms are stabilized by Bi_3In_5 phase in our solder joint. Bi_3In_5 phase is an intermetallic compound phase, and the diffusion of this phase is significantly slower than the diffusion of Bi atoms. Therefore, Bi atoms aggregation slows down, thus a better shear strength can remain and the brittleness of the solder joint can be mitigated after aging. The 140 °C assembly technique brought up in this letter can provide a similar reflow condition to eutectic Sn-Bi solder, while the mechanical performance after aging is much better than Sn-Bi solder. Therefore, the technique is promising to replace the eutectic Sn-Bi solder in advanced electronic packaging.

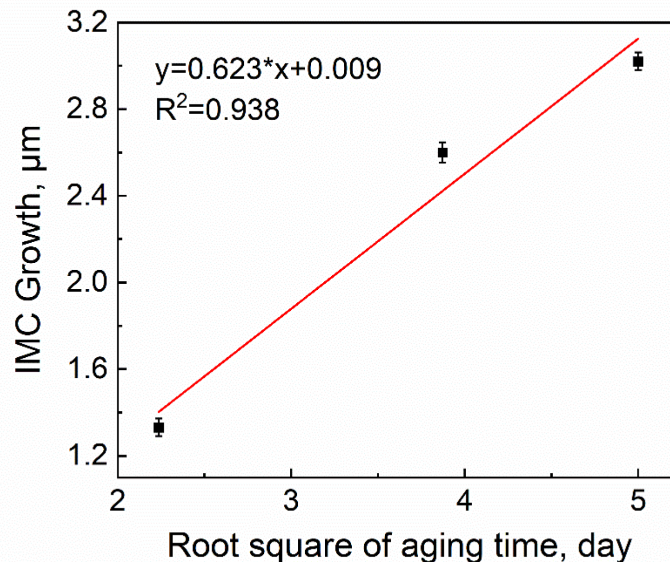

Figure 16. Linear relationship between the thickness of total IMC and the square root of aging days in the fully mixed solder joint.

4. Conclusions

Low-temperature assembly is achieved by reflowing the SAC305 solder ball and 13.5Sn-37.5Bi-45In-4Pb solder paste together at 140 °C for 5 min. The fully mixed solder joint has a uniform microstructure, with two main phases of Bi_3In_5 and γ-phase, and it has very excellent wettability. After 5, 15, and 25 days of aging, the fully mixed solder joint shows a stable microstructure, and there is no continuous aggregation of Bi atoms at the interface between the solder joint and the Cu substrate. More importantly, there is almost no decrease in shear strength after aging for 25 days. The reason is explained as the stabilization effect of Bi atoms by Bi_3In_5 phase, and the IMC did not grow too thick after aging. This technology is promising to replace eutectic Sn-Bi solder in the electronic packaging industry, with a further study on the method of eliminating Pb.

Author Contributions: Conceptualization, Y.L. (Yingxia Liu), Z.G. and L.S.; methodology, Y.L. (Yingxia Liu), X.Z. and L.S.; formal analysis, Y.L. (Yingxia Liu) and L.S.; investigation, L.S.; resources, Y.L. (Yingxia Liu) and Y.L. (Ying Liu); data curation, L.S.; writing—original draft preparation, L.S.; writing—review and editing, Y.L. (Yingxia Liu); visualization, L.S.; supervision, K.T. and Y.L. (Ying Liu); project administration, Y.L. (Yingxia Liu), K.T. and Y.L. (Ying Liu); funding acquisition, Y.L. (Yingxia Liu). All authors have read and agreed to the published version of the manuscript.

Funding: This work was supported by Young Scientists Fund of National Natural Science Foundation of China (grant number 51901022), and the grant from Huawei Technologies (grant number 9239080).

Conflicts of Interest: The authors declare no conflict of interest.

References

1. Gu, S. Material innovation opportunities for 3D integrated circuits from a wireless application point of view. *MRS Bull.* **2015**, *40*, 233–241. [CrossRef]
2. Tu, K.; Liu, Y. Recent advances on kinetic analysis of solder joint reactions in 3D IC packaging technology. *Mater. Sci. Eng. R Rep.* **2018**, *136*, 1–12. [CrossRef]
3. Tu, K. Reliability challenges in 3D IC packaging technology. *Microelectron. Reliab.* **2010**, *51*, 517–523. [CrossRef]
4. Liu, Y.; Li, M.; Kim, D.W.; Gu, S.; Tu, K.N. Synergistic effect of electromigration and Joule heating on system level weak-link failure in 2.5D integrated circuits. *J. Appl. Phys.* **2015**, *118*, 135304. [CrossRef]
5. Mahajan, R.; Sankman, R.; Patel, N.; Kim, D.W.; Aygun, K.; Qian, Z.; Mekonnen, Y.; Salama, I.; Sharan, S.; Iyengar, D.; et al. Embedded Multi-Die Interconnect Bridge (EMIB)—A High Density, High Bandwidth Packaging Interconnect. In Proceedings of the 66th IEEE Electronic Components and Technology Conference (ECTC), Las Vegas, NV, USA, 31 May–3 June 2016; pp. 557–565.
6. Zou, H.; Zhang, Q.; Zhang, Z. Interfacial microstructure and mechanical properties of SnBi/Cu joints by alloying Cu substrate. *Mater. Sci. Eng. A* **2012**, *532*, 167–177. [CrossRef]
7. Song, Q.; Yang, W.; Li, Y.; Mao, J.; Qin, W.; Zhan, Y. Interfacial reaction and mechanical properties of Sn58Bi-XCr solder joints under isothermal aging conditions. *Vacuum* **2021**, *194*, 110559. [CrossRef]
8. Liu, Y.; Ren, B.; Xue, Y.; Zhou, M.; Cao, R.; Zeng, X. Improvement on the mechanical properties of eutectic Sn58Bi alloy with porous Cu addition during isothermal aging. *Mater. Res. Express* **2021**, *8*, 076302. [CrossRef]
9. Mei, Z.; Morris, J.W. Characterization of eutectic Sn-Bi solder joints. *J. Electron. Mater.* **1992**, *21*, 599–607. [CrossRef]
10. Chan, Y.; Lai, J.K.L.; Wu, L.; Poon, N. Residual shear strength of Sn-Ag and Sn-Bi lead-free SMT joints after thermal shock. *IEEE Trans. Adv. Packag.* **2000**, *23*, 708–714. [CrossRef]
11. Liu, P.L.; Shang, J.K. Interfacial embrittlement by bismuth segregation in copper/tin–bismuth Pb-free solder interconnect. *J. Mater. Res.* **2001**, *16*, 1651–1659. [CrossRef]
12. Chen, C.; Ho, C.E.; Lin, A.H.; Luo, G.L.; Kao, C.R. Long-term aging study on the solid-state reaction between 58Bi42Sn solder and Ni substrate. *J. Electron. Mater.* **2000**, *29*, 1200–1206. [CrossRef]
13. Hu, X.; Li, Y.; Min, Z. Interfacial reaction and IMC growth between Bi-containing Sn0.7Cu solders and Cu substrate during soldering and aging. *J. Alloys Compd.* **2014**, *582*, 341–347. [CrossRef]
14. Bi, X.; Hu, X.; Li, Q. Effect of Co addition into Ni film on shear strength of solder/Ni/Cu system: Experimental and theoretical investigations. *Mater. Sci. Eng. A* **2020**, *788*, 139589. [CrossRef]
15. Wang, H.; Hu, X.; Jiang, X. Effects of Ni modified MWCNTs on the microstructural evolution and shear strength of Sn-3.0Ag-0.5Cu composite solder joints. *Mater. Charact.* **2020**, *163*, 110287. [CrossRef]
16. Hu, X.; Xu, T.; Keer, L.M.; Li, Y.; Jiang, X. Microstructure evolution and shear fracture behavior of aged Sn3Ag0.5Cu/Cu solder joints. *Mater. Sci. Eng. A* **2016**, *673*, 167–177. [CrossRef]
17. Zhang, Z.; Hu, X.; Jiang, X.; Li, Y. Influences of mono-Ni (P) and dual-Cu/Ni (P) plating on the interfacial microstructure evolution of solder joints. *Metall. Mater. Trans. A* **2019**, *50*, 480–492. [CrossRef]
18. Zhang, L.; Sun, L.; Guo, Y.H. Microstructures and properties of Sn58Bi, Sn35Bi0.3Ag, Sn35Bi1.0Ag solder and solder joints. *J. Mater. Sci.-Mater. Electron.* **2015**, *26*, 7629–7634. [CrossRef]
19. Morris, J.W.; Goldstein, J.L.F.; Mei, Z. Microstructure and mechanical properties of Sn-In and Sn-Bi solders. *JOM* **1993**, *45*, 25–27. [CrossRef]
20. Han, D.L.; Shen, Y.A.; Huo, F.; Nishikawa, H. Nishikawa, Microstructure Evolution and Shear Strength of Tin-Indium-xCu/Cu Joints. *Metals* **2022**, *12*, 33. [CrossRef]
21. Liu, Y.; Tu, K.N. Low melting point solders based on Sn, Bi, and In elements. *Mater. Today Adv.* **2020**, *8*, 100115. [CrossRef]
22. Xu, R.; Liu, Y.; Sun, F. Effect of isothermal aging on the microstructure, shear behavior and hardness of the Sn58Bi/Sn3.0Ag0.5Cu/Cu solder joints. *Results Phys.* **2019**, *15*, 102701. [CrossRef]
23. Huang, J.Q.; Zhou, M.B.; Zhao, X.F.; Zhang, X.P. Microstructures and shear properties of mixed assembly BGA structure SnAgCu/SnBi(Ag)/Cu joints in board-level packaging. In Proceedings of the 2017 18th International Conference on Electronic Packaging Technology (ICEPT). IEEE, Harbin, China, 16–19 August 2017; pp. 1649–1654.
24. Hadian, F.; Genanu, M.; Owen, R.; Cotts, E.J. The dependence of the microstructure of SnAgCu/SnBiAg mixed assemblies on reflow temperature. In Proceedings of the 2020 SMTA International Conference, Online, 28 September–23 October 2020.
25. Ren, J.; Huang, M.L. Board-level drop reliability and fracture behavior of low temperature soldering Sn–Ag–Cu/Sn–Bi–X hybrid BGA solder joints for consumer electronics. *J. Mater. Sci. Mater. Electron.* **2021**, *32*, 15453–15465. [CrossRef]
26. Wang, F.; Huang, Y.; Du, C. Mechanical properties of SnBi-SnAgCu composition mixed solder joints using bending test. *Mater. Sci. Eng. A* **2016**, *668*, 224–233. [CrossRef]
27. Shen, Y.A.; Zhou, S.; Li, J.; Yang, C.H.; Huang, S.; Lin, S.K.; Nishikawa, H. Sn-3.0Ag-0.5Cu/Sn-58Bi composite solder joint assembled using a low-temperature reflow process for PoP technology. *Mater. Des.* **2019**, *183*, 108144. [CrossRef]
28. Moser, Z.; Dutkiewicz, J.; Gasior, W. *Binary Alloy Phase Diagram*; ASM International: Materials Park, OH, USA, 1990.
29. Kabassis, H.; Rutter, J.W.; Winegard, W.C. Bi-In system: Phase diagram and some eutectic structures. *Met. Sci.* **1984**, *18*, 326–328. [CrossRef]
30. Witusiewicz, V.T.; Hecht, U.; Böttger, B.; Rex, S. Thermodynamic re-optimisation of the Bi-In-Sn system based on new experimental data. *J. Alloys Compd.* **2007**, *428*, 115–124. [CrossRef]

31. Witusiewicz, V.T.; Hecht, U.; Böttger, B.; Rex, S. On the nature of the interface between Ag3Sn intermetallics and sn in Sn-3.5Ag solder alloys. *J. Electron. Mater.* **2007**, *36*, 1615–1620.
32. Lee, C.J.; Min, K.D.; Park, H.J.; Jung, S.B. Mechanical properties of Sn-58 wt% Bi solder containing Ag-decorated MWCNT with thermal aging tests. *J. Alloys Compd.* **2020**, *820*, 153077. [CrossRef]
33. Nai, S.; Wei, J.; Gupta, M. Interfacial intermetallic growth and shear strength of lead-free composite solder joints. *J. Alloys Compd.* **2009**, *473*, 100–106. [CrossRef]
34. Yoon, J.W.; Kim, S.W.; Jung, S.B. IMC growth and shear strength of Sn-Ag-Bi-In/Au/Ni/Cu BGA joints during aging. *Mater. Trans.* **2004**, *45*, 727–733. [CrossRef]
35. Wang, D.; Hao, J.; Zhou, J.; Xue, F.; Tian, S.; Li, S. The influence of thermal aging on reliability of Sn-58Bi interconnects. In Proceedings of the 2017 18th International Conference on Electronic Packaging Technology (ICEPT). IEEE, Harbin, China, 16–19 August 2017; pp. 744–749.
36. Ping, W.U. Effects of Zn addition on mechanical properties of eutectic Sn–58Bi solder during liquid-state aging. *Trans. Nonferrous Met. Soc. China* **2015**, *25*, 1225–1233.
37. Wang, F.; Huang, Y.; Zhang, Z.; Yan, C. Interfacial reaction and mechanical properties of Sn-Bi solder joints. *Materials* **2017**, *10*, 920. [CrossRef] [PubMed]
38. Ahmed, S.; Basit, M.; Suhling, J.C.; Lall, P. IEEE, Effects of Aging on SAC-Bi Solder Materials. In Proceedings of the 15th IEEE Intersociety Conference on Thermal and Thermomechanical Phenomena in Electronic Systems (ITherm), Las Vegas, NV, USA, 31 May–3 June 2016; pp. 746–754.
39. Raeder, C.H.; Felton, L.E.; Tanzi, V.A.; Knorr, D.B. The effect of aging on microstructure, room temperature deformation, and fracture of Sn-Bi/Cu solder joints. *J. Electron. Mater.* **1994**, *23*, 611–617. [CrossRef]